DOI: 10.1002/chem.200701407

Towards a Tunable Tautomeric Switch in Azobenzene Biomimetics: Implications for the Binding Affinity of 2-(4′-Hydroxyphenylazo)benzoic Acid to Streptavidin

Joan-Antoni Farrera,*[a] Ivan Canal,[a] Pedro Hidalgo-Fernández,[a] M. Lluïsa Pérez-García,*[b] Oscar Huertas,[c] and F. Javier Luque*[c]

Abstract: The tautomeric equilibria of 2-(4′-hydroxyphenylazo)benzoic acid (HABA) and 2-(3′,5′-dimethyl-4′-hydroxyphenylazo)benzoic acid (3′,5′-dimethyl-HABA) have been studied by a combination of spectroscopic and computational methods. For neutral HABA in solvents of different polarity (toluene, chloroform, DMSO, DMF, butanol, and ethanol) the azo tautomer (AT) is largely predominant. For monoanionic HABA, the hydrazone tautomer (HT) is the only detected species in apolar solvents such as toluene and chloroform, while the AT is the only detected species in water and a mixture of both tautomers is detected in ethanol. Comparison of the results obtained for HABA and its 3′,5′-dimethylated derivative shows that dimethylation of the hydroxybenzene ring shifts the tautomeric preferences towards the hydrazone species. These findings have been used to examine the differences in binding affinity to streptavidin, as the lower affinity of HABA can be explained in terms of the larger energetic cost associated with the tautomeric shift to the bioactive hydrazone species. Overall, these results suggest that a balanced choice of chemical substituents, embedding environment, and pH can be valuable for exploitation of the azo–hydrazone tautomerism of HABA biomimetics in biotechnological applications.

Keywords: ab initio calculations · azo–hydrazone tautomerism · biomimetics · hydrogen bonds · solvent effects

Introduction

During the past decade the photoisomerization properties of azobenzene derivatives have stimulated research efforts directed towards exploration of their use as materials for digital data storage,[1–5] as central building blocks in molecular rotors,[6,7] and as molecular on–off switches in nanomolecular devices[8] and in ion channels.[9,10] Accordingly, several studies have assessed the structural and spectral properties of *cis* and *trans* isomers of azobenzene compounds and their isomerization mechanism.[11–15] Azobenzene dyes have also been used as biomarkers, due to their ability to undergo azo–hydrazone tautomerism.[16–22] One of the most interesting azobenzene dyes is 2-(4′-hydroxyphenylazo)benzoic acid (HABA), which can bind to proteins such as avidin[23] and streptavidin[24–26] at the same binding site as the natural ligand, biotin,[27] in spite of the structural dissimilarity of these compounds (Scheme 1). At neutral pH, at which HABA exists as a monoanion (HB^-), binding to avidin or streptavidin shifts the absorption band from 347 nm in the free state to 500 nm in the complexed state, which has been interpreted in terms of a change between azo (AT) and hy-

[a] Dr. J.-A. Farrera, I. Canal, P. Hidalgo-Fernández
Departament de Química Orgànica
Facultat de Química
Universitat de Barcelona
Martí i Franqués 1, 08028 Barcelona (Spain)
Fax: (+34) 933397878
E-mail: jfarrera@ub.edu

[b] Dr. M. L. Pérez-García
Departament de Farmacología
i Química Terapèutica
Facultat de Farmàcia, Universitat de Barcelona
Avda. Diagonal 643, 08028 Barcelona (Spain)
Fax: (+34) 93 4021886
E-mail: mlperez@ub.edu

[c] O. Huertas, Prof. Dr. F. J. Luque
Departament de Fisicoquímica
Facultat de Farmàcia
Universitat de Barcelona
Avda. Diagonal 643, 08028 Barcelona (Spain)
Fax: (+34) 93 4035987
E-mail: fjluque@ub.edu

Supporting information for this article is available on the WWW under http://www.chemeurj.org/ or from the author.

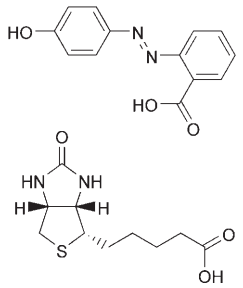

Scheme 1. Representation of HABA (top) and biotin (bottom).

drazone (HT) tautomers in the free and bonded states (Scheme 2).[28] HABA also binds albumin with a shift of the absorption band to 480 nm, which has also been ascribed to the predominance of the HT in the bound state.[29–32] This spectral change forms the basis for a spectrophotometric assay for measuring the ligand-binding activities of avidin and streptavidin solutions.[28,33]

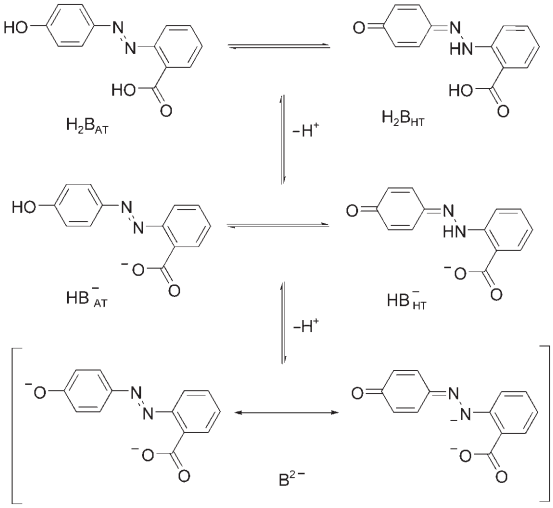

Scheme 2. Acid–base and tautomeric equilibria of HABA.

Understanding of the tautomeric preferences of HABA is important not only for identifying the factors that modulate its binding to proteins, but also for the design of biomimetic compounds with potential biotechnological applications.[25,26] Accordingly, a detailed knowledge of the tautomeric dependence of HABA on both pH and solvation is necessary. However, the available experimental data are controversial. Thus, even though the AT of the neutral species (H_2B) predominates in a variety of organic solvents of different polarity, the main absorption band at 506 nm in DMF has been ascribed to the HT.[34] Moreover, the low solubility of neutral HABA in water precludes the study of its tautomeric equilibration, though this problem can be alleviated by means of co-solvents,[34] or by the addition of an acid or a base.[35] However, it is clear that the predominant tautomer of the cationic (H_3B^+) or anionic (HB^-) species might not necessarily be the same for the neutral form.

This study pursues the examination of the tautomeric equilibria of several 4′-hydroxyphenylazo derivatives (Scheme 3) in order to understand the influence of pH and solvation on the tautomerism of HABA (**3**) and related compounds. The results, which provide a detailed description of the tautomeric preferences of neutral and mono-

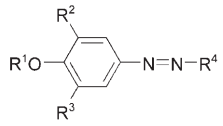

1: R^1=R^2=R^3=H, R^4=CH_3
2: R^1=R^2=R^3=H, R^4=C_6H_5
3: R^1=R^2=R^3=H, R^4=*o*-C_6H_4-CO_2H
4: R^1=R^2=R^3=H, R^4=*p*-C_6H_4-CO_2H
5: R^1=CH_3, R^2=R^3=H, R^4=*o*-C_6H_4-CO_2H
6: R^1=H, R^2=R^3=CH_3, R^4=*o*-C_6H_4-CO_2H

Scheme 3.

anionic species of HABA derivatives, should be valuable for tuning of the biotechnological properties of these compounds.

Results and Discussion

Neutral HABA species (H_2B): To clarify the assignment of the spectroscopic signals of HABA (**3**) to either the AT or the HT, compound **5**, which can only exist in the AT form, was used as reference. The wavelengths of the absorption maxima of **3** and **5** in different media are summarized in Table 1.

Table 1. Wavelengths of the absorption maxima of HABA (**3**) and compounds **5** and **6** in different media.

Solvent	Base/pH	UV/Vis absorption maxima [nm]		
		5	HABA (**3**)	**6**
toluene	–	376	372	391 (450 sh)
	1 equiv DBU	330	471	473
$CHCl_3$	–	378	373	388 (450 sh)
	1 equiv DBU	337	481	479
DMSO	–	342	354	359 and 487
BuOH	–	345	364	480
EtOH	–	350	355	471
	1 equiv DBU	343	350 and 481	481
	70 equiv DBU	343	406	481
H_2O	pH 7.0	345	347[28]	352 and 476[35]
	pH 10.0	345	400	444

Without added base, the UV/Vis spectra of HABA in toluene, chloroform, DMSO, butanol, and ethanol each have an absorption maximum similar to that of **5** in the same solvent, showing that the predominant species in both compounds is the AT. The hypsochromic shift experienced by **3** and **5** on going from apolar solvents (λ_{max} = 372–378 nm) to polar ones (λ_{max} = 342–364 nm) could be explained by increased conjugation of **3** and **5** in apolar solvents, due to an intramolecular hydrogen bond between the carboxylic acid O–H group and the proximal nitrogen atom of the azo group, as noticed in the crystal structure of HABA (**3**).[36] Polar solvents, however, should weaken such a hydrogen bond and possibly favor a more twisted conformation with reduced conjugation.

The data shown in Table 1 cast doubt on the previously reported predominance of the HT of HABA in DMF in the absence of added base.[34] However, since DMF usually contains small amounts of dimethylamine as an impurity, the reported spectrum of HABA in DMF might correspond to the monoanion (HB^-) instead of the neutral species (H_2B). To check this hypothesis, the UV/Vis absorption spectrum of HABA in analytical grade DMF was recorded, and a main absorption band at 352 nm and a less intense band at 506 nm were observed. Addition of triethylamine to this solution increased the 506 nm band at the expense of the 352 nm one, while addition of acetic acid had the reverse effect. These results therefore point to the AT (λ_{max} = 352 nm) being the predominant species of neutral HABA in DMF, and so the absorption band at 506 nm should be assigned to the HT of the monoanion (HB^-_{HT}).

To gain further insight into the tautomerism of neutral HABA, theoretical calculations were first performed to determine the intrinsic tautomeric preferences of **1**, **2**, and **4**, in which the relative stabilities between the ATs and the HTs are simply modulated by the natures of the R^4 substituent (CH_3 in **1**, C_6H_5 in **2**, *p*-C_6H_5-CO_2H in **4**; see Scheme 4 and Table 2). In the case of **1** the AT is nearly planar, but in the HT the methyl group is twisted around 15 degrees due to the pyramidalization of the nitrogen atom bonded to the methyl group, which thus minimizes the steric repulsion between the hydrazone N–H group and the benzene C–H unit *ortho* to the azo group (H···H distance of 2.02 Å). In contrast, both the ATs and the HTs adopt planar geometries in **2** and **4**, which reflects the stabilizing effects due to the extended conjugation of the molecules. In the case of compound **1**, the AT is around 13 kcal mol^{-1} more stable than the HT both in the gas phase and in solution (Table 2). Replacement of methyl (**1**) by phenyl (**2**) reduces the relative stability gap between AT and HT by 3 kcal mol^{-1}, but the latter species is still disfavored (by ca. 10 kcal mol^{-1}). Finally, addition of a carboxylic group at the *para* position of the benzene ring (**4**) leads to a very slight stabilization (by 0.5–1.1 kcal mol^{-1}) of the hydrazone species (Table 2).

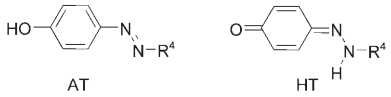

Scheme 4. Representation of the azo (AT) and hydrazone (HT) tautomers in compounds **1**, **2**, and **4**.

The tautomerism in HABA was explored by consideration of eight different azo–hydrazone species, shown in Scheme 5. In contrast with the results obtained for **4**, the structure of HABA deviates significantly from planarity, even though twisting of the chemical skeleton varies between the different tautomers (Table 3). The repulsion between the lone pairs of the N_{azo} and O_{COOH} atoms in **AT I** and **AT III** provides grounds for the deviation of the *o*-carboxybenzene ring from planarity, while the twisting in **AT IV** is related to the formation of the seven-membered hydrogen-bonded ring. In **AT II**, the small twisting observed in the azo unit can be attributed, at least in part, to the N_{azo}···H–O_{COOH} hydrogen bond (N···O distance: 2.66 Å). As a result, **AT II** is found to be the most stable azo tautomer, being favored by more than 2 kcal mol^{-1} relative to the

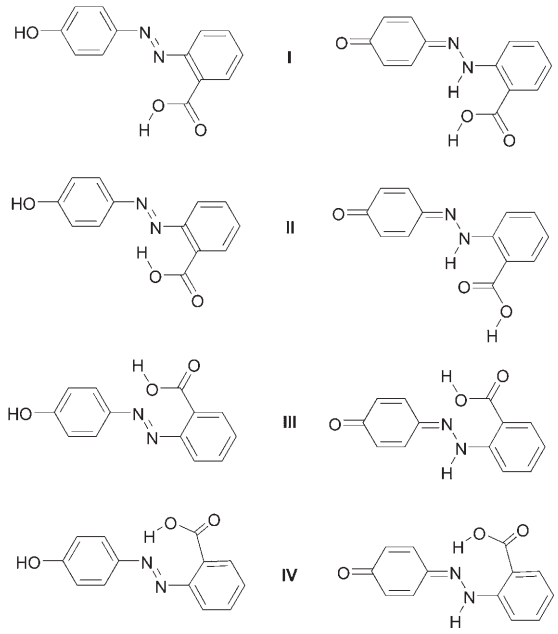

Scheme 5. Representation of the azo and hydrazone species considered in the tautomeric equilibrium of HABA (**3**).

Table 2. Selected geometrical parameters for the azo and hydrazone tautomers of compounds **1**, **2**, and **4**, and free energy differences[a] (at 298 K; kcal mol^{-1}) in the gas phase and in solution.

Compound	Tautomer	Geometrical parameters[b]			Relative stability[c]				
		τ_1	τ_2	τ_3	Gas	CCl_4	$HCCl_3$	Octanol	Water
1	AT	−179.9	180.0	–	0.0	0.0	0.0	0.0	0.0
(R^4=CH_3)	HT	179.1	164.2	–	13.4	13.9	13.3	13.2	12.8
2	AT	180.0	180.0	0.0	0.0	0.0	0.0	0.0	0.0
(R^4=C_6H_5)	HT	180.0	180.0	0.0	10.5	11.0	10.3	10.1	9.3
4	AT	180.0	180.0	0.0	0.0	0.0	0.0	0.0	0.0
(R^4=*p*-C_6H_5–CO_2H)	HT	180.0	180.0	0.0	10.0	10.5	9.5	9.3	8.2

[a] See Scheme 4 for nomenclature. The most stable *trans* orientation of the substituent R^4 (relative to the benzene ring) was considered in computations. [b] Dihedral angles (degrees) are defined as τ_1: N8-N7-C1-C2; τ_2: C9-N8-N7-C1; τ_3: C10-C9-N8-N7. [c] Values determined from MP2/aug-cc-pVDZ+[CCSD-MP2/6-31G(d)] calculations in the gas phase, and combined with the relative solvation free energies to estimate the relative stability in solution. In all cases the azo tautomer is used as reference.

Table 3. Selected geometrical parameters for the azo and hydrazone tautomers of HABA (**3**), and free energy differences (at 298 K; kcal mol^{-1}) in the gas phase and in solution.

Tautomer[a]	Geometrical parameters[b]					Relative stability[c]				
	τ_1	τ_2	τ_3	τ_4	d_{YH}/d_{YX}	Gas	CCl_4	$HCCl_3$	Octanol	Water
	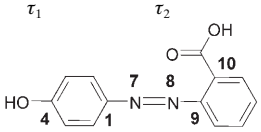									
AT I	−170.6	178.5	−32.3	148.5	–	2.4	2.8	2.8	2.7	1.5
AT II	−165.0	−178.2	2.2	−175.1	1.75/2.66	0.0	0.0	0.0	0.0	0.0
AT III	174.2	177.3	−30.7	135.1	–	2.3	2.5	2.4	2.3	1.0
AT IV	173.7	179.0	29.1	147.7	1.70/2.63	7.8	7.7	7.6	7.5	7.3
HT I	180.0	180.0	0.0	180.0	1.88/2.66	6.1	7.6	7.6	8.0	8.0
HT II	180.0	180.0	0.0	180.0	1.86/2.68	3.2	5.1	5.5	6.2	6.6
HT III	175.7	179.9	32.9	136.5	–	13.6	14.5	13.6	13.4	11.4
HT IV	−179.6	−163.9	60.2	144.2	1.78/2.70	16.7	17.1	16.2	15.9	14.8

[a] See Scheme 5 for nomenclature. [b] Dihedral angles (degrees) are defined as τ_1: N8-N7-C1-C2; τ_2: C9-N8-N7-C1; τ_3: C10-C9-N8-N7; τ_4: O(=C)-C-C10-C9. Lengths (Å) of the intramolecular X−H···Y hydrogen bonds (left: H···Y; right: X···Y). [c] Values determined from MP2/aug-cc-pVDZ+[CCSD-MP2/6-31G(d)] calculations in the gas phase, and combined with the relative solvation free energies to estimate the relative stability in solution.

other azo species in the gas phase, even though the relative stabilities between tautomers with (**AT II**) and without (**AT I** and **AT III**) intramolecular hydrogen bonds decrease as the polarity of the solvent is increased. For the hydrazone forms, while **HT III** and **HT IV** strongly deviate from planarity, the most favored species—**HT I** and **HT II**—are planar, due to the $N_{hydrazone}$–H···O_{COOH} hydrogen bond (Table 3), which also explains the higher stability of these forms.

The azo form **AT II** is more stable than the hydrazone species **HT II** by 3.2 kcal mol^{-1} in the gas phase. Comparison with the results obtained for **4** (Table 2) shows that moving the carboxylic group from the *para* position (**4**) to the *ortho* position (**3**) has a dramatic effect on the tautomerism, since the azo form is destabilized by around 6 kcal mol^{-1}. However, solvation tends to stabilize the azo form of neutral HABA (see Table 3), and the population of the hydrazone species can be expected to decrease significantly as the polarity of the solvent is increased. Overall, in agreement with the spectroscopic data, these results indicate that the neutral form of HABA should mainly exist as the azo tautomer **AT II**.

Monoanionic species of HABA (HB^-): Since the second pK_a value of HABA in water is 8.2,[37] at neutral pH HABA exists as a monoanion. The similarity between the spectra found for **3** and **5** in water at neutral pH (λ_{max} = 345–347 nm; Table 1) indicates that the predominant species of the monoanionic HABA is the AT.[35]

In contrast, a completely different tautomeric scenario is seen in chloroform or toluene. When 1 equiv of DBU was added to a solution of **5**, the absorption maximum at 337 (chloroform) or 330 nm (toluene) revealed the formation of a new species, which corresponds to the AT of the monoanion (Table 1). In contrast, when 1 equiv of DBU was added to a chloroform solution of HABA, the absorption band was shifted to 481 nm (Figure 1), a wavelength similar to that of HABA complexed to avidin or albumin, which was assigned to the HT. A similar absorption band (λ_{max} = 471 nm) appeared after addition of DBU to a solution of HABA in toluene. Addition of large excesses (1000 equiv) of DBU to solutions of **3** and **5** in chloroform did not cause any further change in the UV/Vis spectra, which means that DBU is not basic enough to generate the dianionic species of HABA. Likewise, addition of 5 equiv of a weak base such as imidazole led only to a small decrease in absorbance, without any shift in the absorption band, which indicates that imidazole is not basic enough to deprotonate the carboxylic acid group and generate the monoanionic species.

To confirm that the 481 nm absorption band was due to the HT of monoanionic HABA, the Raman spectra of **3** and **5** under similar experimental conditions were recorded. As expected, the Raman spectrum of the anion of **5** contained a band at 1416 cm^{-1} assigned to the N=N stretching,[35] while no significant bands were found near 1615 cm^{-1}. However, the Raman spectrum of the monoanion of HABA featured an intense band at 1624 cm^{-1}, which can be attributed to the HT, but no band was detected near 1400 cm^{-1} (Figure 1). Overall, these findings support the supposition that the HT is the predominant tautomer of the monoanionic HABA in chloroform and toluene.

The different tautomeric behavior observed for HABA in chloroform (or toluene) and in water, where the HT and the AT predominate, respectively, led us to investigate its tautomeric preferences in ethanol, which has an intermediate polarity. DBU was therefore added to an ethanolic solution of **5** to generate its anion, which can only exist as the AT, and the absorption maximum (343 nm) was similar to that of the anion in water and after addition of DBU to a chloroform solution (Table 1). Nevertheless, when either 1 equiv of DBU or a large excess of DABCO were added to an ethanolic solution of HABA, the absorption band split into two bands at 350 and 481 nm, which should be attributable to the AT and the HT, respectively (Figure 2). The monoanion

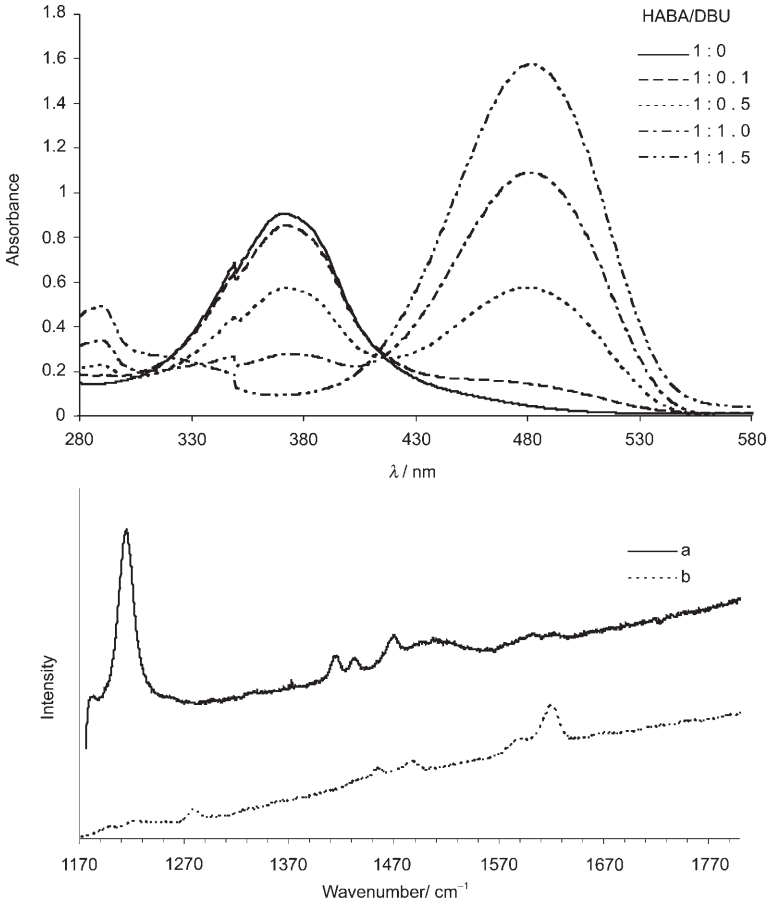

Figure 1. Top) UV/Vis titration of HABA (4.0×10^{-5} M in chloroform) with DBU. Bottom) Raman spectra of equimolar mixtures of a) **5** and DBU in chloroform ($c=1.6\times10^{-3}$ M), and b) HABA (**3**) and DBU in chloroform ($c=8.0\times10^{-4}$ M). Excitation wavelength: 488 nm.

of HABA in ethanol thus exists as a mixture of both tautomers, an intermediate situation between that found in chloroform and in water.

Unlike in chloroform, DBU (but not DABCO) in ethanolic medium is basic enough to generate the dianion of HABA. Thus, on addition of an excess of DBU to the monoanion of HABA in ethanol, the absorption bands of the two tautomers (350 and 481 nm) were transformed into a single band at 406 nm corresponding to the dianion (Figure 2). This assignment is supported by the similar wavelength of the absorption maximum of HABA in water at pH 10 ($\lambda_{max}=400$ nm), in which the dianion should be the main species.

To explore the main tautomers of monoanionic HABA further, the relative stabilities of azo and hydrazone species (Scheme 6) were determined by theoretical computations. For the HT, however, only one hydrazone form (**HT V**) was considered, since geometry optimization of **HT VI** yielded **HT V**, as would be expected in view of the stabilizing contribution due to the hydrogen bond between the hydrazone N–H group and the carboxylic oxygen, which favors a planar structure (see Table 4). In contrast, the optimized structure of the azo tautomers exhibits a large twisting due to the repulsion between the lone pairs of nitrogen (azo) and oxygen (carboxy) atoms.

HT V is the most stable form in the gas phase, the azo species being destabilized by around 15 kcal mol^{-1} (see Table 4). Solvation, however, has an enormous influence on the tautomerism, since the preference for the hydrazone species is drastically reduced as the polarity of the solvent increases, and **AT V** is then predicted to be slightly more stable (by 0.7 kcal mol^{-1}) in aqueous solution. This latter finding was corroborated by additional cluster-continuum computations[38] in which two water molecules were specifically placed around the carboxylate group (data not shown), thus providing supporting evidence for the reversal of the tautomeric preference in water, which agrees with the experimental data reported in Table 1.

In summary, both experimental and theoretical results agree in predicting that the monoanionic form of HABA mainly populates the hydrazone species **HT V** except in the most polar solvent (water), in which the azo species **AT V** is the main tautomeric form.

Neutral and monoanionic species of the 3′,5′-dimethylated derivative 6: The tautomeric equilibrium of **6** is more favorable than that of HABA to the HT (see Table 1). Thus, for the neutral species, whereas the AT is still the predominant form in apolar solvents, the HT is also detectable as a shoulder around 450 nm. Moreover, single absorption bands at 471–480 nm are observed for **6** in polar solvents, and should be assigned to the HT form.

The tautomerism of the monoanionic form of **6** is also more favorable to the HT than in the case of HABA. Thus, single absorption bands between 473 and 481 nm were found in toluene, chloroform, and ethanol, and should be assigned to the HT. Only in water at pH values between 5 and 8 were mixtures of both AT ($\lambda_{max}=352$ nm) and HT ($\lambda_{max}=476$ nm) found.[35] On increasing the pH, these two bands were transformed into a single band with $\lambda_{max}=444$ nm, which should correspond to the dianion (Figure 3). In ethanol solution, a very large excess of DBU was required to generate a similar absorption band ($\lambda_{max}=454$ nm) attributable to the dianion of **6**.

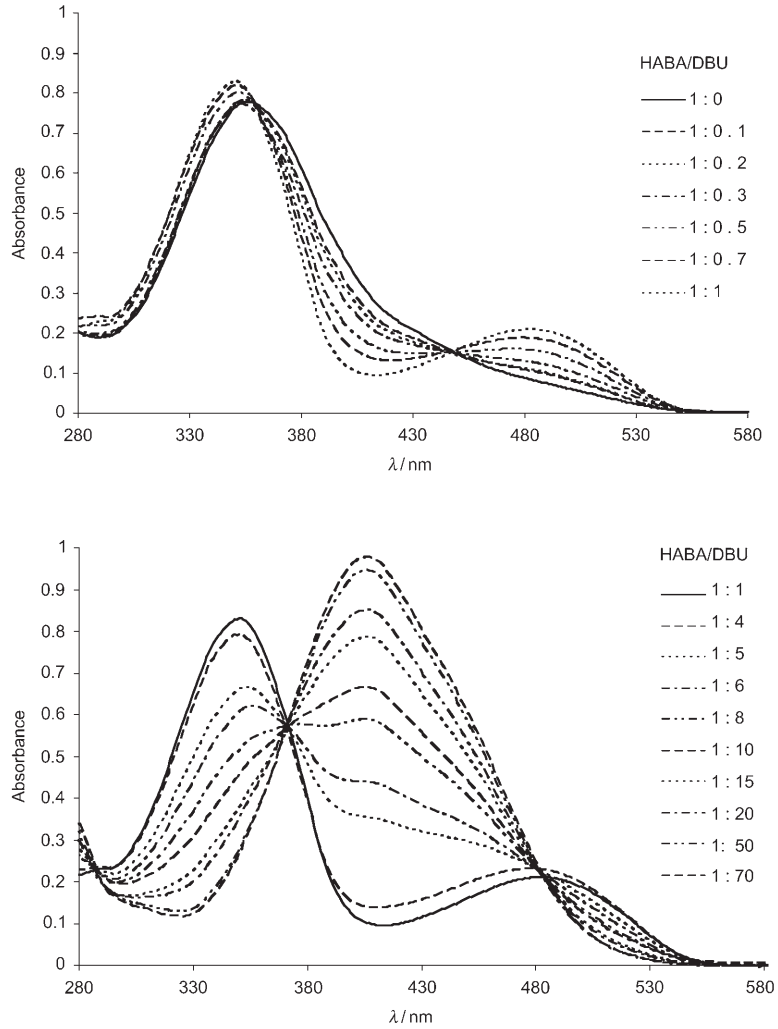

Figure 2. UV/Vis titration of HABA (3.6×10^{-5} M in ethanol) with DBU.

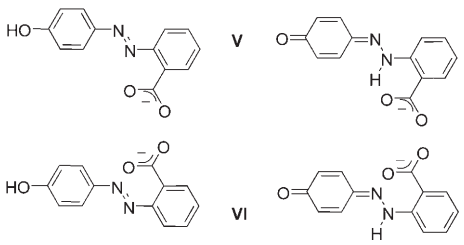

Scheme 6. Representation of the azo and hydrazone species considered in the tautomeric equilibrium of monoanionic HABA (**3**).

Both experimental and theoretical results demonstrate that the tautomeric scenario for HABA is extremely sensitive to the nature of the solvent and to the ionization state of the compound. In the neutral compound, HABA mainly exists as the azo tautomer **AT II**. However, upon deprotonation, the monoanionic form of HABA turns out to populate the hydrazone species **HT V**, even though the relative stability between azo and hydrazone forms is drastically reduced in the most polar solvents. In fact, the azo species **AT V** is the main tautomeric form in aqueous solution (see Table 1), which can be explained by water-induced destabilization of the intramolecular hydrogen bond formed between the N–H group and the carboxylate anion in the hydrazone tautomer. Accordingly, in addition to the switching strategies that rely on the photochemical *cis* ⇄ *trans* isomerization of azobenzene derivatives, these compounds could also be exploitable as molecular switches by triggering azo ⇄ hydrazone tautomerism through a simple chemical effector such as (de)-protonation under suitable environmental conditions.

Chemical modification also exerts a notable influence on the azo–hydrazone tautomerism. Though the results obtained for the neutral HABA and its isomeric compound **4** indicate that the AT is the main tautomer in the two cases, the intrinsic (gas-phase) tautomeric preference of the AT in **4** is diminished by around 6 kcal mol^{-1} when the carboxylic group is attached to the *ortho* position in HABA. This effect can be attributed to the different energetic stabilization originating from the intramolecular hydrogen bonds formed in both AT (**AT II**) and HT (**HT II**), where the nitrogen atom of the azo/hydrazone group acts as hydrogen bond acceptor and donor, respectively (see Scheme 5). Accordingly, it can be expected that the relative stability between azo and hydrazone tautomers should be modulatable by manipulation of the relative strengths of those hydrogen bonds. At this point, it is worth noting that the strength of related resonance-assisted hydrogen bonding[39,40] can be affected not only by altering the nature of the hydrogen bond donor and acceptor groups, but also through the aromaticity of the benzene ring,[41–43] thus opening the possibility of influencing the tautomeric preference by chemical modification of the aromatic system with both donor and acceptor atoms.

Besides chemical modification at the carboxybenzene unit, here we have also explored the effect of a different chemical modification, which consists of the dimethylation of the phenolic ring of HABA. The results indicate that this apparently minor chemical change has a delicate, but clear,

Table 4. Selected geometrical parameters for the azo and hydrazone tautomers of monoanionic HABA (**3**), and free energy differences (at 298 K; kcal mol^{-1}) in the gas phase and in solution.

Tautomer[a]	Geometrical parameters[b]					Relative stability[c]				
	τ_1	τ_2	τ_3	τ_4	d_{YH}/d_{YX}	Gas	CCl_4	$HCCl_3$	Octanol	Water
AT V	152.1	176.9	19.7	−137.6	–	15.5	10.5	7.3	4.3	−0.7
AT VI	138.6	−173.8	34.6	38.9	–	18.6	17.9	17.7	16.6	15.3
HT V	180.0	180.0	180.0	0.0	1.53/2.52	0.0	0.0	0.0	0.0	0.0

[a] See Scheme 6 for nomenclature. [b] Dihedral angles (degrees) are defined as τ_1: N8-N7-C1-C2; τ_2: C9-N8-N7-C1; τ_3: C10-C9-N8-N7; τ_4: O(=C)-C-C10-C9. Lengths (Å) of the intramolecular X−H···Y hydrogen bonds (top: H···Y; bottom: X···Y). [c] Values determined from MP2/aug-cc-pVDZ+[CCSD-MP2/6-31G(d)] calculations in the gas phase, and combined with the relative solvation free energies to estimate the relative stability in solution.

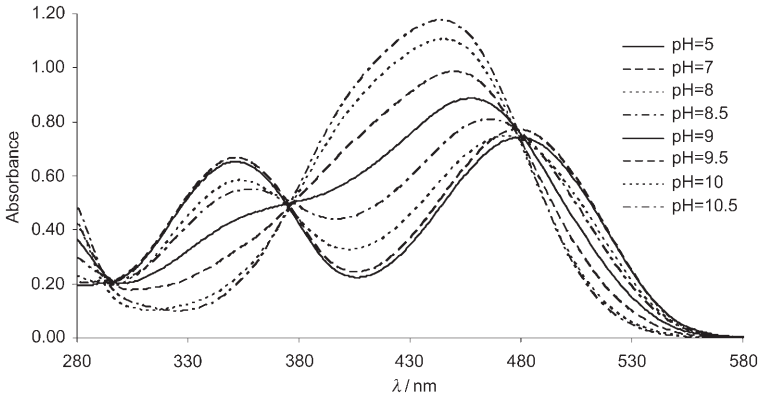

Figure 3. UV/Vis spectra of 3′,5′-dimethyl-HABA (**6**) [5.3×10^{-5} M in phosphate buffer (0.1 M)] at different pH values.

influence on the azo–hydrazone tautomerism of HABA, as noted in the fact that both azo and hydrazone tautomers are detected for the monoanionic form of **6** in aqueous solution, whereas the monoanion of HABA is found to exist only in the azo form (see Table 1). This effect can be attributed to the steric hindrance between the methyl substituents at positions 3′ and 5′ and the hydroxy group of the azo tautomer of HABA. In turn, these findings suggest that the balance between azo and hydrazone tautomers of azobenzene derivatives can be altered through the incorporation of specific functional groups into suitably preorganized azobenzene scaffolds, thus paving the way to tune the biotechnological applications of these compounds.

On the basis of the preceding discussion, it is worth revisiting the differences between HABA and its 3′,5′-dimethylated derivative **6** in their binding affinities towards streptavidin in light of their azo–hydrazone tautomerism, as the subtle, but distinctive, trends in the tautomeric preferences of these compounds could play a role in modulating their binding affinities. HABA binds to streptavidin with minimal alteration of the binding site geometry (see ref. [26] for details). One of the benzoate oxygen atoms of HABA occupies the same position as the biotin ureido oxygen, and the carboxylate anion forms several interactions with Asn23, Ser27, Tyr43, and Ser45, thus mimicking the network of interactions found for biotin. The remainder of the linked ring system of HABA delineates the orientation of the fused biotin ring and valerate side chain. However, whereas the terminal carboxylate group of the valerate chain interacts with Asn49 and Ser88, the hydroxybenzene unit of HABA does not form specific contacts with protein residues, but a stacking interaction with the indole ring of Trp79. These trends might explain why HABA does not completely immobilize the loop comprising residues 46–50, in contrast with the binding of biotin. A similar interaction pattern has also been reported for the complex formed between HABA and avidin,[23,44] and for the binding of 3′,5′-dimethyl HABA to streptavidin.[24,25,44]

The low-dielectric protein environments that define the binding sites in avidin or streptavidin have been assumed to bind the hydrazone form of monoanionic HABA,[25,26] which should correspond to the species **HT V**. However, as our results also indicate that the monoanion of HABA in aqueous solution mainly exists as the azo tautomer **AT V**, binding to streptavidin implies an energetic penalty due to a tautomeric change between free (azo) and complexed (hydrazone) states. This detrimental contribution to the binding affinity should be less significant for 3′,5′-dimethyl HABA (**6**), due to the displacement of the tautomeric equilibrium towards the hydrazone species (see above), thus enhancing binding to streptavidin. In fact, this conclusion is supported by the experimentally determined binding affinities of **3** and **6** (−5.27 and −8.29 kcal mol^{-1},[25,26] respectively), which indicates that the dimethylated derivative binds to streptavidin around 160 times better than HABA does (binding constants of 7.3×10^{3} M^{-1} for **3** and 1.2×10^{6} M^{-1} for **6**). Interestingly, this ratio agrees with the difference between the relative stabilities of azo (**AT V**) and hydrazone (**HT V**) species determined in aqueous solution for the monoanion of

HABA (-0.7 kcal mol^{-1}; see Table 4) and of its 3′,5′-dimethylated derivative **6** ($+1.9$ kcal mol^{-1}; see Table S1 in the Supporting Information).

The fact that HABA binds to avidin and streptavidin (binding constants of 1.7×10^{5} M^{-1} and 7.3×10^{3} M^{-1}, respectively) as the HT prompted us to investigate the binding affinity of a HABA derivative that lacked the capability to tautomerize to HT. For that purpose, compound **5**, which can only exist as the AT, was used. By means of a competition experiment with HABA, compound **5** was found to bind to avidin with a binding constant approximately two orders of magnitude lower than that of HABA (see Supporting Information), which gives support to the biological implications of the tautomerism between the AT and the HT in mediating the binding affinities of HABA and related compounds. According to these results, it is reasonable to expect that derivatives of HABA with a labile protecting group on the phenolic hydroxy group—which, like compound **5**, could only exist in their azo tautomeric forms—should have low binding affinities for avidin and streptavidin. Deprotection of the phenolic hydroxy group under mild conditions would then unfreeze the azo–hydrazone tautomerism, leading to a ligand with a high binding affinity for those proteins. In this way, a mild deprotection step could trigger the azo→hydrazone tautomerism, increasing the interest of these compounds as switches of the binding affinity towards avidin and streptavidin.

In the context of the preceding discussion, it can be concluded that the introduction of suitable substituents and labile protecting groups, together with the embedding of HABA in environments of different polarity and pH, can be regarded as valuable strategies for modulation of the balance between azo and hydrazone species, and in turn for switching of binding affinities to avidin and streptavidin. These strategies might contribute to exploitation of the biotechnological applications of HABA biomimetics.

Conclusion

The tautomeric equilibration of 2-(4′-hydroxyphenylazo)-benzoic acid (HABA) and its derivatives is strongly influenced by the protonation state (neutral vs. monoanionic) of the compound, the polarity of the medium, and the substitution pattern on the hydroxyphenyl ring and presumably on the carboxybenzene moiety. Both spectroscopic and computational data indicate that the tautomerism behavior of the monoanion of HABA is more complex than that of the neutral species. Thus, whereas the azo form **AT II** is found to be the main species of the neutral HABA in all the solvents, its monoanion exists predominantly as the hydrazone species **HT V** in apolar solvents, but the tautomeric preference changes to the azo tautomer **AT V** as the polarity of the solvent is increased. Moreover, these results also indicate that on increasing the substitution on the hydroxyphenyl ring, as in 3′,5′-dimethyl-HABA (**6**), there is a tendency to favor the HT. This trend should explain the better binding affinity of this latter compound, which mainly stems from a decrease in the energy cost required to bind the bioactive tautomer.

In conclusion, the introduction of appropriate substituents and labile protecting groups, and the embedding of HABA in environments of different polarity and pH, can be regarded as valuable strategies with which to modulate the biotechnological applications of azobenzene biomimetics.

Experimental Section

General: NMR spectra were obtained with a Varian–Gemini spectrometer (200 MHz for ^{1}H and 50.3 MHz for ^{13}C) and a Varian–Mercury spectrometer (400 MHz for ^{1}H and 100 MHz for ^{13}C) at 25 °C. Chemical shifts are reported in ppm relative to TMS as internal standard. UV/Vis spectra were recorded with a Varian CARY 500 spectrophotometer. Infrared spectra were recorded with a FT-IR Nicolet instrument. Mass spectra were recorded on a ZQ Micromass instrument for ES spectra, a HP-5988 A instrument for CI spectra, and a VG-QUATTRO Micromass instrument for FAB spectra. Raman spectra were recorded on a Jobin Yvon T64000 Raman spectrophotometer with use of the 488.0 nm excitation line of a Coherent INNOVA 300 Ar^{+} laser. pH values were measured on a Cyberscan 510 pH-meter. Melting points were determined on a Kofler Reichert Thermovar instrument with polarized light and are not corrected.

Anhydrous chloroform was obtained by distillation from potassium carbonate and filtered through activated basic alumina. DMSO was purified by partial freezing. The water used in UV measurements was purified in a Millipore system (Milli-Q). All others solvents were dried and purified by standard procedures described in the literature.[45]

Methyl 2-(4′-methoxyphenylazo)benzoate: This compound was synthesized from HABA by a literature procedure[46] in 71 % yield. ^{1}H NMR as described; ^{13}C NMR (50.3 MHz, [D$_6$]DMSO): $\delta=168.1$, 162.9, 151.2, 146.7, 132.5, 130.4, 129.7, 129.0, 125.4, 119.8, 115.3, 56.3, 52.9 ppm; IR (KBr): $\tilde{\nu}=3070$, 2925, 1717, 1252 cm^{-1}; MS-FAB (+): m/z: 271.4 $[M+H]^{+}$, 239.3 $[M-31]^{+}$.

2-(4′-Methoxyphenylazo)benzoic acid (5): This compound was synthesized from methyl 2-(4′-methoxyphenylazo)benzoate by a literature procedure[46] in 76 % yield. M.p. 150–153 °C (lit.[46] 149–150 °C); ^{1}H NMR as described; ^{13}C NMR (50.3 MHz, [D$_6$]DMSO): $\delta=169.0$, 163.0, 151.2, 147.0, 132.1, 131.0, 130.4, 123.0, 125.5, 118.5, 115.3, 56.4 ppm; EM-CI (+): m/z: 256.0 $[M]^{+}$, 134.9 $[M-CH_3OC_6H_4N]^{+}$.

2-(4′-Hydroxy-3′,5′-dimethylphenylazo)benzoic acid (6): This compound was synthesized by coupling the diazonium salt of 2-aminobenzoic acid to 2,6-dimethylphenol, by a general method reported in the literature,[25,35] in 46 % yield. M.p. 190–192 °C; ^{1}H NMR (200 MHz, [D$_6$]DMSO): $\delta=2.24$ (s, 6H; CH_3), 7.48–7.76 ppm (m; 6H); EM-CI (+): m/z: 270.0 $[M]^{+}$, 149.0 $[M-C_6H_4CO_2H]^{+}$, 121.0 $[M-N_2C_6H_2(CH_3)_2OH]^{+}$.

Computational details: Full geometry optimizations were performed at the MP2/6-31G(d) level. The natures of the stationary points were verified by inspection of the vibrational frequencies within the harmonic oscillator approximation, which were positive in all cases. Single-point MP2/aug-cc-pVDZ calculations were subsequently performed to determine the relative energy differences between tautomers, and the contributions of higher-order electron correlation effects were estimated from the differences between CCSD and MP2 energies by use of the 6-31G(d) basis set. The best estimates of the energy differences between stationary points was determined by combining the relative energies computed at the MP2/aug-cc-pVDZ level and the differences between the energies obtained from CCSD and MP2 calculations. Zero point, thermal, and entropic corrections evaluated within the framework of the harmonic oscillator-rigid rotor at 1 atm and 298 K were added to the relative energies to obtain the free energy differences in the gas phase. To estimate the influence of solvation, QM SCRF continuum calculations were performed by using the HF/6-31G(d) (neutral compounds) and HF/6-31+G(d) (ionic species) optimized versions of the MST model,[47,48] which is based

on the polarizable continuum model.[49,50] The relative stabilities in solution were estimated by combining the free energy difference in the gas phase and the differences in free energy of solvation determined from MST calculations. Gas-phase calculations were carried out with Gaussian 03.[51] MST calculations were performed with a locally modified version of Monstergauss.[51]

Acknowledgement

This research was supported by the Generalitat de Catalunya (2005SGR000653, 2005SGR00158, and 2005SGR00286) and by the Spanish Ministerio de Ciencia y Tecnologia (BQU2002–02424, FIS2006–03525, TEC2005–07996-C02–02/MIC, and CTQ2005–08797-C02–01/BQU).

[1] A. Natansohn, P. Rochon, X. Meng, C. Barrett, T. Buffeteau, S. Bonenfant, M. Pezolet, *Macromolecules* **1998**, *31*, 1155–1161.
[2] G. Pace, V. Ferri, C. Grave, M. Elbing, C. von Haenisch, M. Zharnikov, M. Mayor, M. A. Rampi, P. Samori, *Proc. Natl. Acad. Sci. USA* **2007**, *104*, 9937–9942.
[3] P. H. Rasmussen, P. S. Ramanujam, S. Hvilsted, R. H. Berg, *J. Am. Chem. Soc.* **1999**, *121*, 4738–4743.
[4] N. K. Viswanathan, D. Y. Kim, S. Bian, J. Williams, W. Liu, L. Li, L. Samuelson, J. Kumar, S. K. Tripathy, *J. Mater. Chem.* **1999**, *9*, 1941–1955.
[5] A. Natansohn, P. Rochon, *Chem. Rev.* **2002**, *102*, 4139–4175.
[6] D.-H. Qu, Q.-C. Wang, J. Ren, H. Tian, *Org. Lett.* **2004**, *6*, 2085–2088.
[7] H. Murakami, A. Kawabuchi, K. Kotoo, M. Kunitake, N. Nakashima, *J. Am. Chem. Soc.* **1997**, *119*, 7605–7606.
[8] S. Loudwig, H. Bayley, *J. Am. Chem. Soc.* **2006**, *128*, 12404–12405.
[9] M. Volgraf, P. Gorostiza, S. Szobota, M. R. Helix, E. Y. Isacoff, D. Trauner, *J. Am. Chem. Soc.* **2007**, *129*, 260–261.
[10] M. Volgraf, P. Gorostiza, R. Numano, R. H. Kramer, E. Y. Isacoff, D. Trauner, *Nat. Chem. Biol.* **2006**, *2*, 47–52.
[11] P.-O. Aastrand, P. S. Ramanujam, S. Hvilsted, K. L. Bak, S. P. A. Sauer, *J. Am. Chem. Soc.* **2000**, *122*, 3482–3487.
[12] L. Briquet, D. P. Vercauteren, E. A. Perpete, D. Jacquemin, *Chem. Phys. Lett.* **2006**, *417*, 190–195.
[13] H. Fliegl, A. Koehn, C. Haettig, R. Ahlrichs, *J. Am. Chem. Soc.* **2003**, *125*, 9821–9827.
[14] N. Tamaoki, M. Wada, *J. Am. Chem. Soc.* **2006**, *128*, 6284–6285.
[15] T. Tsuji, H. Takashima, H. Takeuchi, T. Egawa, S. Konaka, *J. Phys. Chem. A* **2001**, *105*, 9347–9353.
[16] G. Gabor, Y. F. Frei, E. Fischer, *J. Phys. Chem.* **1968**, *72*, 3266–3272.
[17] P. Jacques, H. Strub, J. See, J. P. Fleury, *Tetrahedron* **1979**, *35*, 2071–2073.
[18] N. Kurita, S. Nebashi, M. Kojima, *Chem. Phys. Lett.* **2005**, *408*, 197–204.
[19] A. Lycka, D. Snobl, V. Machacek, M. Vecera, *Org. Magn. Reson.* **1981**, *16*, 17–19.
[20] A. Lycka, D. Snobl, V. Machacek, M. Vecera, *Org. Magn. Reson.* **1981**, *15*, 390–393.
[21] M. Nepras, M. Titz, M. Necas, S. Lunak, Jr., R. Hrdina, A. Lycka, *Collect. Czech. Chem. Commun.* **1988**, *53*, 213–226.
[22] H. Zollinger, *Color chemistry: syntheses, properties and applications of organic dyes and pigments*, VCH, Weinheim, **1991**.
[23] O. Livnah, E. A. Bayer, M. Wilchek, J. L. Sussman, *FEBS Lett.* **1993**, *328*, 165–168.
[24] P. C. Weber, *Acta Crystallogr. Sect. D* **1995**, *51*, 590–596.
[25] P. C. Weber, M. W. Pantoliano, D. M. Simons, F. R. Salemme, *J. Am. Chem. Soc.* **1994**, *116*, 2717–2724.
[26] P. C. Weber, J. J. Wendoloski, M. W. Pantoliano, F. R. Salemme, *J. Am. Chem. Soc.* **1992**, *114*, 3197–3200.
[27] P. C. Weber, D. H. Ohlendorf, J. J. Wendoloski, F. R. Salemme, *Science* **1989**, *243*, 85–88.
[28] N. M. Green, *Biochem. J.* **1965**, *94*, C23.
[29] J. H. Baxter, *Arch. Biochem. Biophys.* **1964**, *108*, 375–383.
[30] I. Moriguchi, S. Fushimi, C. Ohshima, N. Kaneniwa, *Chem. Pharm. Bull.* **1970**, *18*, 2447–2452.
[31] J. B. Pedersen, S. M. Pedersen, W. E. Lindup, *Biochem. Pharmacol.* **1989**, *38*, 3485–3490.
[32] E. W. Thomas, J. C. Merlin, *Spectrochim. Acta Part A* **1979**, *35*, 1251–1255.
[33] J.-A. Farrera, P. Hidalgo-Fernandez, J. M. Hannink, J. Huskens, A. E. Rowan, N. A. J. M. Sommerdijk, R. J. M. Nolte, *Org. Biomol. Chem.* **2005**, *3*, 2393–2395.
[34] M. R. Mahmoud, S. A. Ibrahim, M. A. Hamed, *Spectrochim. Acta Part A* **1983**, *39 A*, 729–733.
[35] J. C. Merlin, E. W. Thomas, *Spectrochimica Acta Part A* **1979**, *35*, 1243–1249.
[36] H. Qian, W. Huang, *J. Mol. Struct.* **2005**, *743*, 191–195.
[37] I. M. Klotz, H. A. Fiess, J. Y. C. Ho, M. Mellody, *J. Am. Chem. Soc.* **1954**, *76*, 5136–5140.
[38] J. R. Pliego, Jr., J. M. Riveros, *J. Phys. Chem. A* **2002**, *106*, 7434–7439.
[39] G. Gilli, F. Bellucci, V. Ferretti, V. Bertolasi, *J. Am. Chem. Soc.* **1989**, *111*, 1023–1028.
[40] P. Gilli, V. Bertolasi, L. Pretto, A. Lycka, G. Gilli, *J. Am. Chem. Soc.* **2002**, *124*, 13554–13567.
[41] T. M. Krygowski, J. E. Zachara, B. Osmialowski, R. Gawinecki, *J. Org. Chem.* **2006**, *71*, 7678–7682.
[42] M. Palusiak, S. Simon, M. Sola, *J. Org. Chem.* **2006**, *71*, 5241–5248.
[43] P. Sanz, O. Mo, M. Yanez, J. Elguero, *J. Phys. Chem. A* **2007**, *111*, 3585–3591.
[44] S. Repo, T. A. Paldanius, V. P. Hytoenen, T. K. M. Nyholm, K. K. Halling, J. Huuskonen, O. T. Pentikaeinen, K. Rissanen, J. P. Slotte, T. T. Airenne, T. A. Salminen, M. S. Kulomaa, M. S. Johnson, *Chem. Biol.* **2006**, *13*, 1029–1039.
[45] D. D. Perrin, W. L. F. Armarego, *Purification of laboratory chemicals*, Butterworth Heinemann, Oxford, **1996**.
[46] S. Zbaida, C. F. Brewer, W. G. Levine, *Drug Metab. Dispos.* **1994**, *22*, 412–418.
[47] C. Curutchet, A. Bidon-Chanal, I. Soteras, M. Orozco, F. J. Luque, *J. Phys. Chem. B* **2005**, *109*, 3565–3574.
[48] C. Curutchet, M. Orozco, F. J. Luque, *J. Comput. Chem.* **2001**, *22*, 1180–1193.
[49] S. Miertus, E. Scrocco, J. Tomasi, *Chem. Phys.* **1981**, *55*, 117–129.
[50] S. Miertus, J. Tomasi, *Chem. Phys.* **1982**, *65*, 239–245.
[51] *Gaussian 03*, *Revision B.04*, M. J. Frisch, G. W. Trucks, H. B. Schlegel, G. E. Scuseria, M. A. Robb, J. R. Cheeseman, J. A. Montgomery, Jr., T. Vreven, K. N. Kudin, J. C. Burant, J. M. Millam, S. S. Iyengar, J. Tomasi, V. Barone, B. Mennucci, M. Cossi, G. Scalmani, N. Rega, G. A. Petersson, H. Nakatsuji, M. Hada, M. Ehara, K. Toyota, R. Fukuda, J. Hasegawa, M. Ishida, T. Nakajima, Y. Honda, O. Kitao, H. Nakai, M. Klene, X. Li, J. E. Knox, H. P. Hratchian, J. B. Cross, C. Adamo, J. Jaramillo, R. Gomperts, R. E. Stratmann, O. Yazyev, A. J. Austin, R. Cammi, C. Pomelli, J. W. Ochterski, P. Y. Ayala, K. Morokuma, G. A. Voth, P. Salvador, J. J. Dannenberg, V. G. Zakrzewski, S. Dapprich, A. D. Daniels, M. C. Strain, O. Farkas, D. K. Malick, A. D. Rabuck, K. Raghavachari, J. B. Foresman, J. V. Ortiz, Q. Cui, A. G. Baboul, S. Clifford, J. Cioslowski, B. B. Stefanov, G. Liu, A. Liashenko, P. Piskorz, I. Komaromi, R. L. Martin, D. J. Fox, T. Keith, M. A. Al-Laham, C. Y. Peng, A. Nanayakkara, M. Challacombe, P. M. W. Gill, B. Johnson, W. Chen, M. W. Wong, C. Gonzalez, J. A. Pople, Gaussian, Inc., Pittsburgh PA, **2003**.

Received: September 6, 2007
Published online: December 27, 2007

